BBA - Molecular Basis of Disease 1865 (2019) 1284–1297

Contents lists available at ScienceDirect

BBA - Molecular Basis of Disease

journal homepage: www.elsevier.com/locate/bbadis

Chronic kidney disease induced by an adenine rich diet upregulates integrin linked kinase (ILK) and its depletion prevents the disease progression

Sergio de Frutos[a,b,c], Alicia Luengo[a,b,c], Andrea García-Jérez[a,b,c], Marco Hatem-Vaquero[a,b,c], Mercedes Griera[a,b,c], Francisco O'Valle[f], Manuel Rodríguez–Puyol[a,b,c], Diego Rodríguez–Puyol[b,c,d,e,1], Laura Calleros[a,b,c,*,1]

[a] Department of Systems Biology, Universidad de Alcalá, Alcalá de Henares, Madrid, Spain
[b] IRSIN, IRYCIS (Instituto de Salud Carlos III), Madrid, Spain
[c] REDinREN (Instituto de Salud Carlos III), Madrid, Spain
[d] Department of Medicine, Universidad de Alcalá, Alcalá de Henares, Madrid, Spain
[e] Department of Nephrology Section and Research Foundation, Hospital Universitario Príncipe de Asturias, Alcalá de Henares, Madrid, Spain
[f] Departamento de Anatomía Patológica e Historia de la Ciencia, Universidad de Granada, Granada, Spain

ARTICLE INFO

Keywords:
Chronic renal disease
Integrin-linked kinase
Tubulointerstitial damage
Fibrosis
Epithelial-to-mesenchymal transition
Inflammation

ABSTRACT

Kidney fibrosis is one of the main pathological findings of progressive chronic kidney disease (CKD) although the pathogenesis of renal scar formation remains incompletely explained. Integrin-linked kinase (ILK), a major scaffold protein between the extracellular matrix (ECM) and intracellular signaling pathways, is involved in several pathophysiological processes during renal damage. However, ILK contribution in the CKD progress remains to be fully elucidated. In the present work, we studied 1) the renal functional and structural consequences of CKD genesis and progression when ILK is depleted and 2) the potential of ILK depletion as a therapeutic approach to delay CKD progression. We induced an experimental CKD model, based on an adenine-supplemented diet on adult wild-type (WT) and ILK-depleted mice, with a tubulointerstitial damage profile resembling that is observed in human CKD. The adenine diet induced in WT mice a progressive increase in plasma creatinine and urea concentrations. In the renal cortex it was also observed tubular damage, interstitial fibrosis and progressive increased ECM components, pro-inflammatory and chemo-attractant cytokines, EMT markers and TGF-β1 expressions. These observations were highly correlated to a simultaneous increase of ILK expression and activity. In adenine-fed transgenic ILK-depleted mice, all these changes were prevented. Additionally, we evaluated the potential role of ILK depletion to be applied after the disease induction, as an effective approach to interventions in human CKD subjects. In this scenario, two weeks after the establishment of adenine-induced CKD, ILK was abrogated in WT mice and stabilized renal damage, avoiding CKD progression. We propose ILK to be a potential target to delay renal disease progression.

1. Introduction

Chronic kidney disease (CKD) is currently a worldwide health problem with rising incidence and poor outcomes. It is characterized by the sustained and progressive, decline of glomerular filtration rate, which is conditioned by the excessive accumulation of extracellular matrix (ECM) proteins at the extracellular compartment, both at glomerular and tubule-interstitial levels. The mechanisms responsible for this increased ECM protein synthesis seem to be very complex, but it appears to relay mainly in the tissue inflammation that characterizes some of the renal diseases [1,2], and in the transformation of resident renal cells into matrix producing cells [3,4]. In addition, and concerning specially to the development of tubule-interstitial fibrosis, some authors propose that the transformation of renal epithelial and endothelial cells toward a mesenchymal state, through the epithelial-to-mesenchymal (EMT) or endothelial-to-mesenchymal transition process, may also contribute to ECM deposition in the extracellular compartment [5,6]. As these mechanisms have not been definitely demonstrated, it has been also suggested that tubular epithelial cells would relay signals to the underlying interstitial compartment, thus promoting myofibroblast differentiation

* Corresponding author at: Department of Systems Biology, Physiology Unit, Facultad de Medicina, Universidad de Alcalá, Campus Universitario s/n, Alcalá de Henares 28871, Madrid, Spain.
E-mail address: laura.calleros@uah.es (L. Calleros).
[1] Both authors shared senior direction of this work.

https://doi.org/10.1016/j.bbadis.2019.01.024
Received 5 September 2018; Received in revised form 21 December 2018; Accepted 23 January 2019
Available online 03 February 2019

Table 1
Parameters of wild type (WT) and ILK conditional-knockdown (cKD-ILK) mice fed with standard or adenine-rich diet during 6 weeks.

Parameters	0 week	2 weeks	4 weeks	6 weeks
Body weight (g)				
WT Control	25.9 ± 3.5	30.1 ± 1.6	27.8 ± 3.4	28.6 ± 4.7
cKD-ILK Control	25.2 ± 3.5	26.7 ± 2.4	26.5 ± 3.2	27.2 ± 3.2
WT Adenine	25.1 ± 2.4	19.8 ± 3.8$^{*\#}$	20.3 ± 4.8$^{*\#}$	20.1 ± 2.1$^{*\#}$
cKD-ILK Adenine	24.4 ± 2.8	22.2 ± 1.6$^{*\#}$	22.1 ± 2.8$^{*\#}$	21.3 ± 1.7$^{*\#}$
Mean arterial pressure (mmHg)				
WT Control	88.7 ± 1	88.9 ± 0.8	89.5 ± 1.1	90.7 ± 2.2
cKD-ILK Control	88.7 ± 0.6	87.9 ± 1.3	88.8 ± 0.6	88.9 ± 0.8
WT Adenine	87.1 ± 0.8	93 ± 7.3	110.1 ± 8$^{*\#}$	128.0 ± 9.7$^{*\#}$
cKD-ILK Adenine	87.9 ± 1.2	91.5 ± 3.5	90.8 ± 2.8$^{\$}$	93.6 ± 2.4$^{*\$}$

Body weights (g) and mean arterial pressures (mmHg) of WT and cKD-ILK mice fed with standard (Control) or adenine-rich diet (Adenine) during 0, 2, 4 or 6 weeks. n = 10 animals/group. All values are represented as mean ± SEM. *P < 0.05 vs. 0 week, $^{\#}$P < 0.05 vs. WT or cKD-ILK Controls at the same time, $^{\$}$P < 0.05 vs. WT Adenine at the same time.

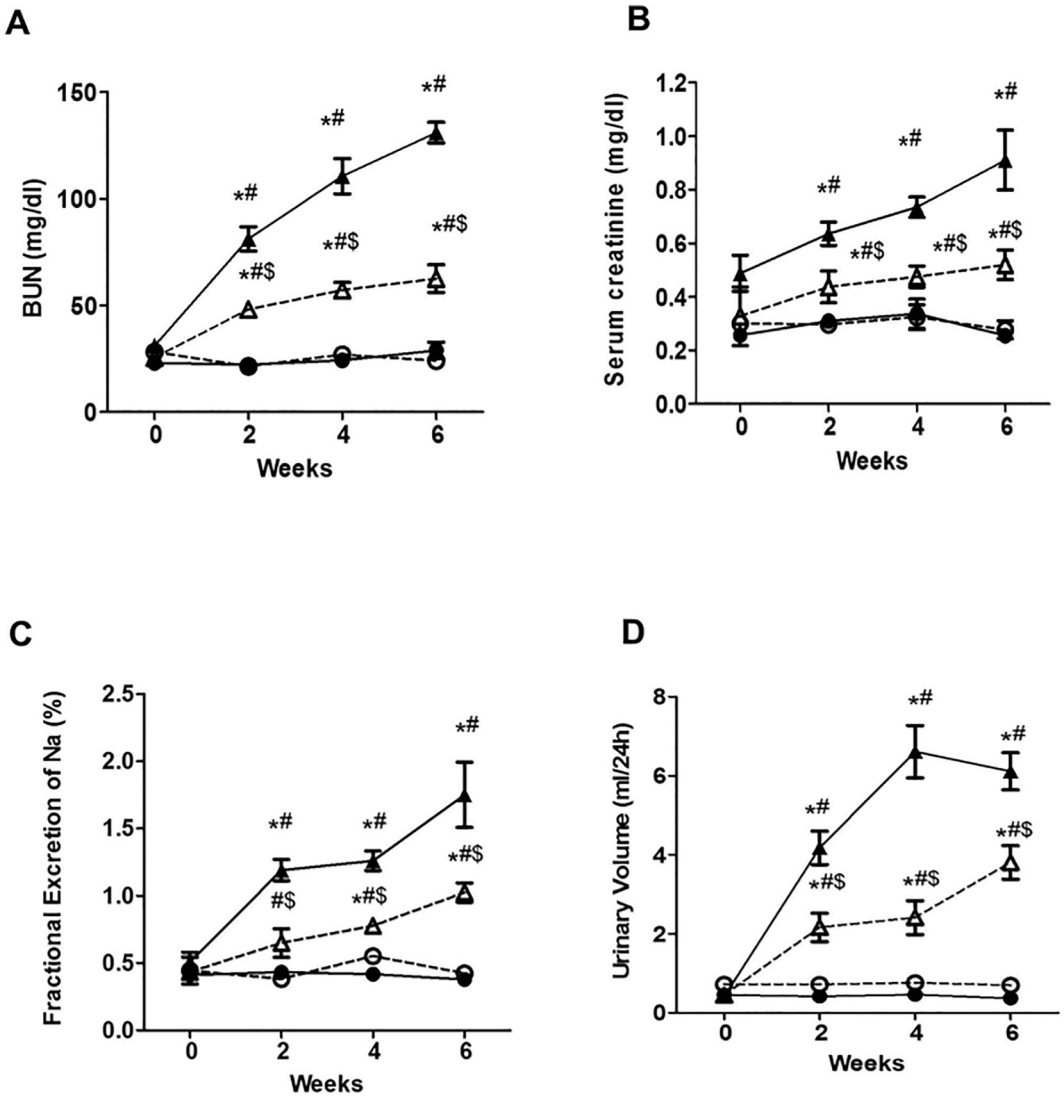

Fig. 1. ILK depletion improves renal function in adenine-fed mice.
Wild type (WT, continuous lines, black symbols) and ILK conditional-knockdown (cKD-ILK, dashed lines, open symbols) mice were fed an adenine-rich diet (triangles) or standard diet as control (circles) during 0, 2, 4 or 6 weeks. Renal function was assessed by measuring serum (A) blood urea nitrogen (BUN) and (B) creatinine (mg/dl), (C) Fractional excretion of Na (%), and (D) urinary volume (μl/24 h). n = 10 animals/group. Results shown are the mean ± SEM. *P < 0.05 vs. 0 week, $^{\#}$P < 0.05 vs. WT or cKD-ILK controls at the same time, $^{\$}$P < 0.05 vs. WT Adenine at the same time.

and immune cells recruitment with the subsequently increased fibrogenesis and inflammation [6–8].

Integrin-linked kinase (ILK) is a key intracellular component of the integrin signaling complex that functions as a scaffold molecule and as a serine/threonine protein kinase that links cell-membrane matrix adhesion receptors (integrins) to actin cytoskeleton and to numerous

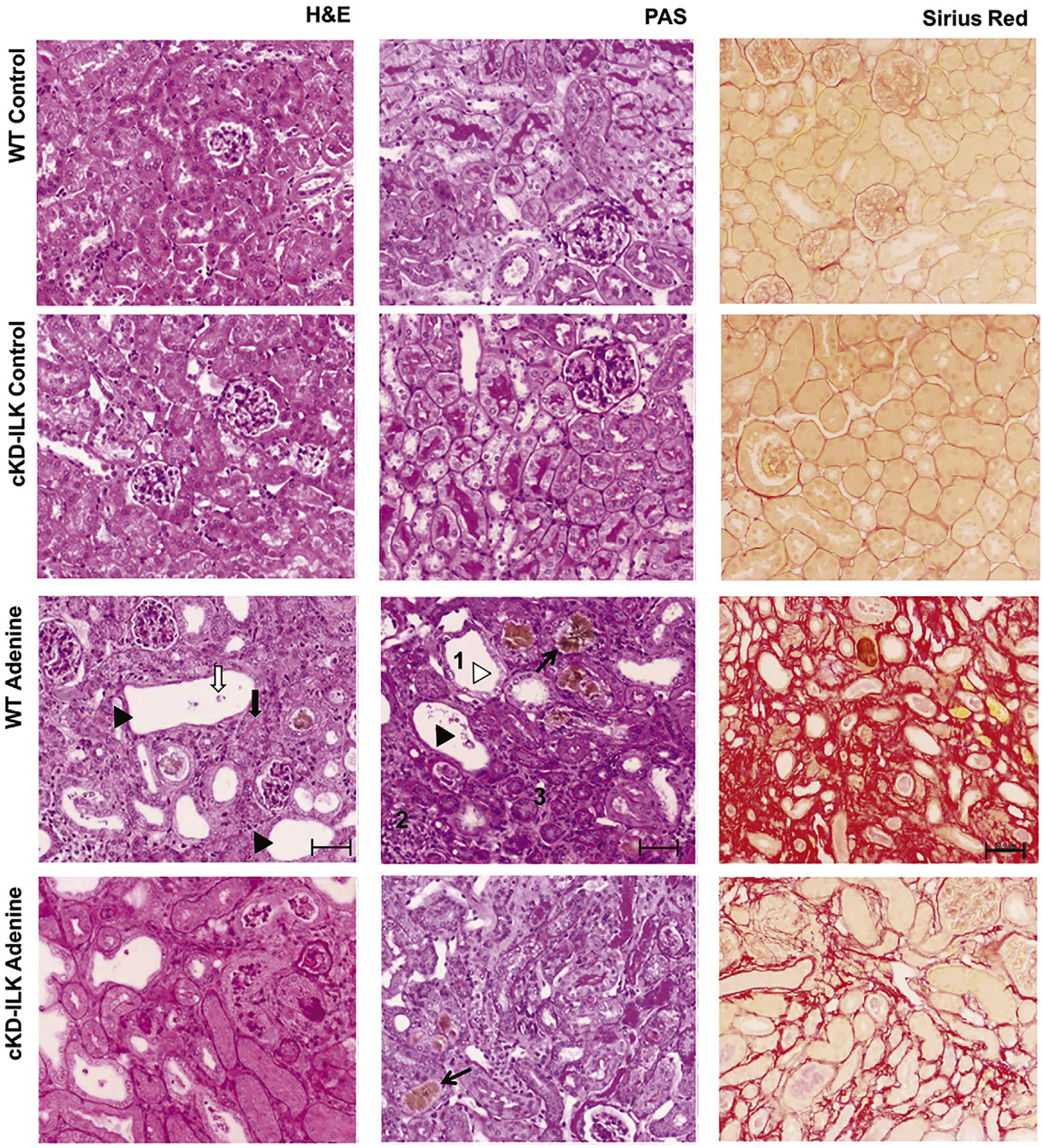

Fig. 2. ILK depletion protects against tubule-interstitial renal damage and decreases interstitial fibrosis development in adenine-fed mice.
Wild type (WT) and ILK conditional-knockdown (cKD-ILK) mice were fed an adenine-rich diet or standard diet as control for 6 weeks and renal cortex samples were histologically analyzed in original ×200 magnifications. Scale bars represent 50 μm. Representative photomicrographs of H&E, PAS and Sirius Red stainings. Numbers and symbols in the WT-Adenine group mark representative tubular dilation (1), inflammation (2) and atrophy (3), tubular epithelial loss (black arrowheads), brush border loss (white arrowheads) and apoptosis (white arrows) and pus casts in tubules (black arrows). Adenine crystals within tubules (open head black arrows) are also shown. The analyzed scores of n = 10 animals per group are displayed in Table 2.

intracellular signaling pathways [9–11]. ILK-downstream effectors include glycogen synthase kinase 3β (GSK-3β), protein kinase B (PKB/AKT) and mitogen-activated protein kinases (MAPKs) [12]. ILK is fundamental in survival, proliferation/apoptosis, differentiation, cell adhesion, migration, invasion and ECM deposition [9,11,13,14]. Upregulation of ILK expression and/or activity has been implicated in the pathogenesis of a wide variety of chronic kidney diseases as a mediator during the nephrotic syndrome [15], proteinuria [16,17], podocyte damage [17,18] and diabetic nephropathy [19,20]. Moreover, other authors point to ILK as a key mediator in renal interstitial fibrogenesis and EMT induced by a range of stimuli, including TGF-β1 [21,22], connective tissue growth factor [23] and high glucose levels [17,19,24]. Recently, we demonstrated that ILK depletion in vivo diminishes the expression of EMT marker α-SMA and the inducer TGF-β1, in renal tubular epithelial cells of a cisplatin-induced acute kidney injury model [25]. The mechanisms followed by ILK to promote EMT includes the related to renal fibrosis, and they are executed by specific EMT-TFs such as Snail and Twist, which downregulate the expression of the epithelial marker E-cadherin [19,21,22,26].

In addition, our group demonstrated that abnormally high levels of

Table 2
Analysis of the histological changes observed in kidneys of wild type (WT) and ILK conditional-knockdown (cKD-ILK) mice fed with standard or adenine-rich diets during 6 weeks.

Group	Tubular dilatation	Loss of tubular epithelial cells	Loss of brush border in PT	Tubular Apoptosis	Tubular atrophy	Pus casts in tubules	Interstitial Inflammation	Interstitial fibrosis
WT Control	0.0 (0-0)	0.0 (0-0)	0.0 (0-0)	0.0 (0-0)	0.0 (0-0)	0.0 (0-0)	0.0 (0-0)	1.01 ± 0.2
cKD-ILK Control	0.0 (0-0)	0.0 (0-0)	0.0 (0-0)	0.0 (0-0)	0.0 (0-0)	0.0 (0-0)	0.0 (0-0)	0.83 ± 0.1
WT Adenine	2 (1-3)$^{\#}$	1 (1-2)$^{\#\$}$	1 (1-2)$^{\#}$	2 (1-2)$^{\#}$	1 (1-2)$^{\#}$	2 (2-3)$^{\#}$	2 (1-2)$^{\#}$	241.8 ± 42.6$^{\#}$
cKD-ILK Adenine	1 (1-2)$^{\#}$	1 (0-1)$^{\#\$}$	1 (0-1)$^{\#\$}$	1 (0-1)$^{\#\$}$	1 (0-1)$^{\#\$}$	1 (0-1)$^{\#\$}$	1 (0-2)$^{\#\$}$	19.1 ± 18.5$^{\#\$}$

WT and cKD-ILK mice were fed with adenine-rich or standard (Control) diets. The 6th week of treatment, kidney sections were stained with Hematoxylin–eosin and the following histopathological features were quantitatively different scored according to the grade of affected renal area (0 to 3); Tubular dilatation, loss of tubular epithelial cells, loss of brush border in proximal tubules (PT), tubular apoptosis, tubular atrophy, pus casts in tubules and interstitial inflammation, and the median scores are represented. Interstitial fibrosis was assessed by Sirius red staining of the collagen renal cortex content and represented as mean ± SEM (relative units). n = 10 animals/group. $^{\#}P < 0.05$ vs. WT or cKD-ILK controls at the same time, $^{\$}P < 0.05$ vs. WT Adenine at the same time.

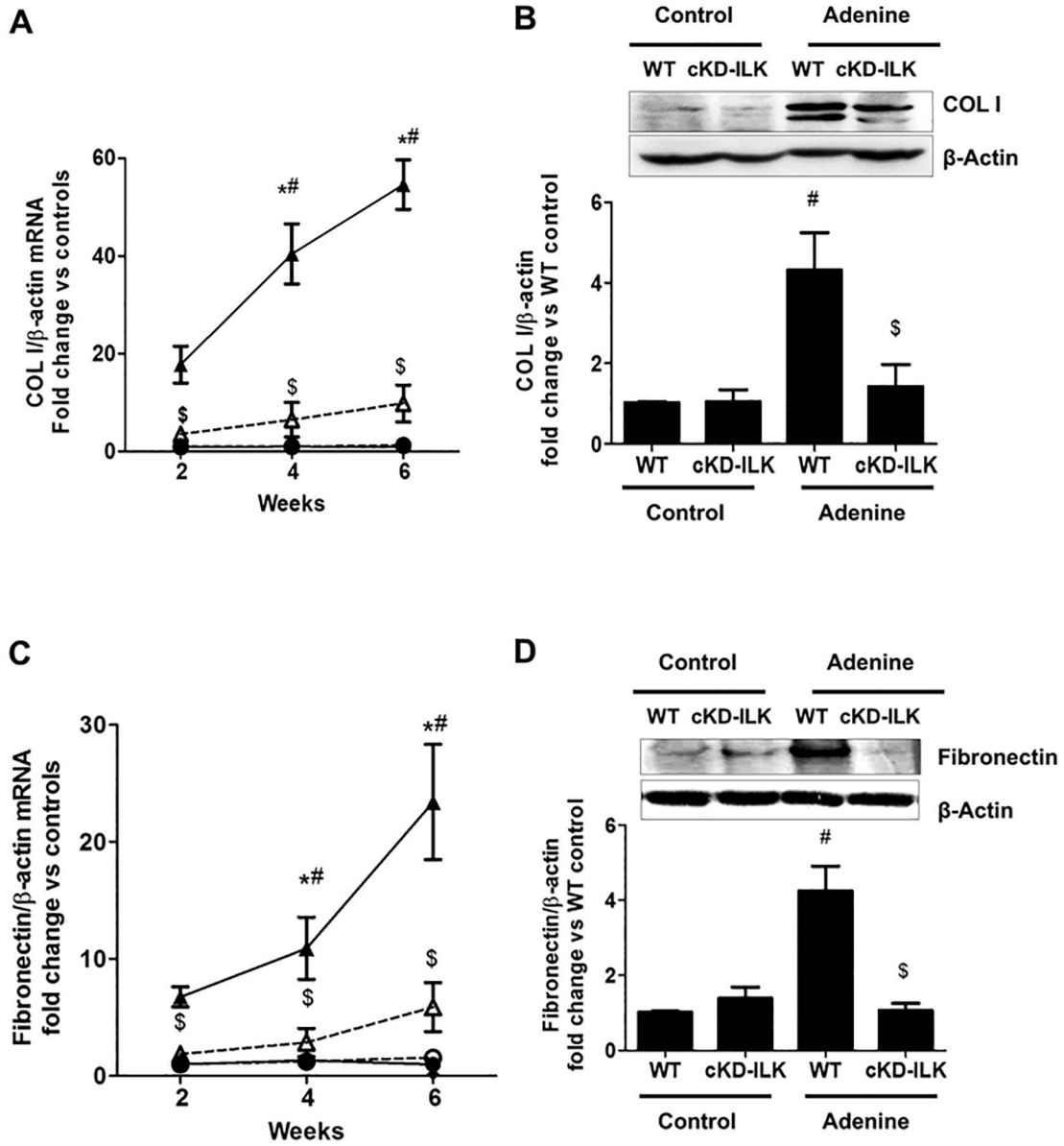

Fig. 3. ILK depletion prevents extracellular matrix protein accumulation in the renal cortex of adenine-fed mice.
Wild type (WT, continuous lines, black symbols) and ILK conditional-knockdown (cKD-ILK, dashed lines, open symbols) mice were fed an adenine-rich (triangles) or standard diet (controls, circles) during 2, 4 or 6 weeks and renal cortex samples were analyzed. Collagen I (COL I) (A) mRNA expression and (B) 6th week protein content and fibronectin (C) mRNA expression and (D) 6th week protein content were quantified. Relative fold changes in mRNA or protein content vs. control WT are represented after the normalization with total β-actin content as the endogenous control. Results are shown as mean ± SEM. *P < 0.05 vs. 2 weeks, $^{\#}P < 0.05$ vs. WT or cKD-ILK controls at the same time, $^{\$}P < 0.05$ vs. WT Adenine at the same time. (n = 10 animals/group).

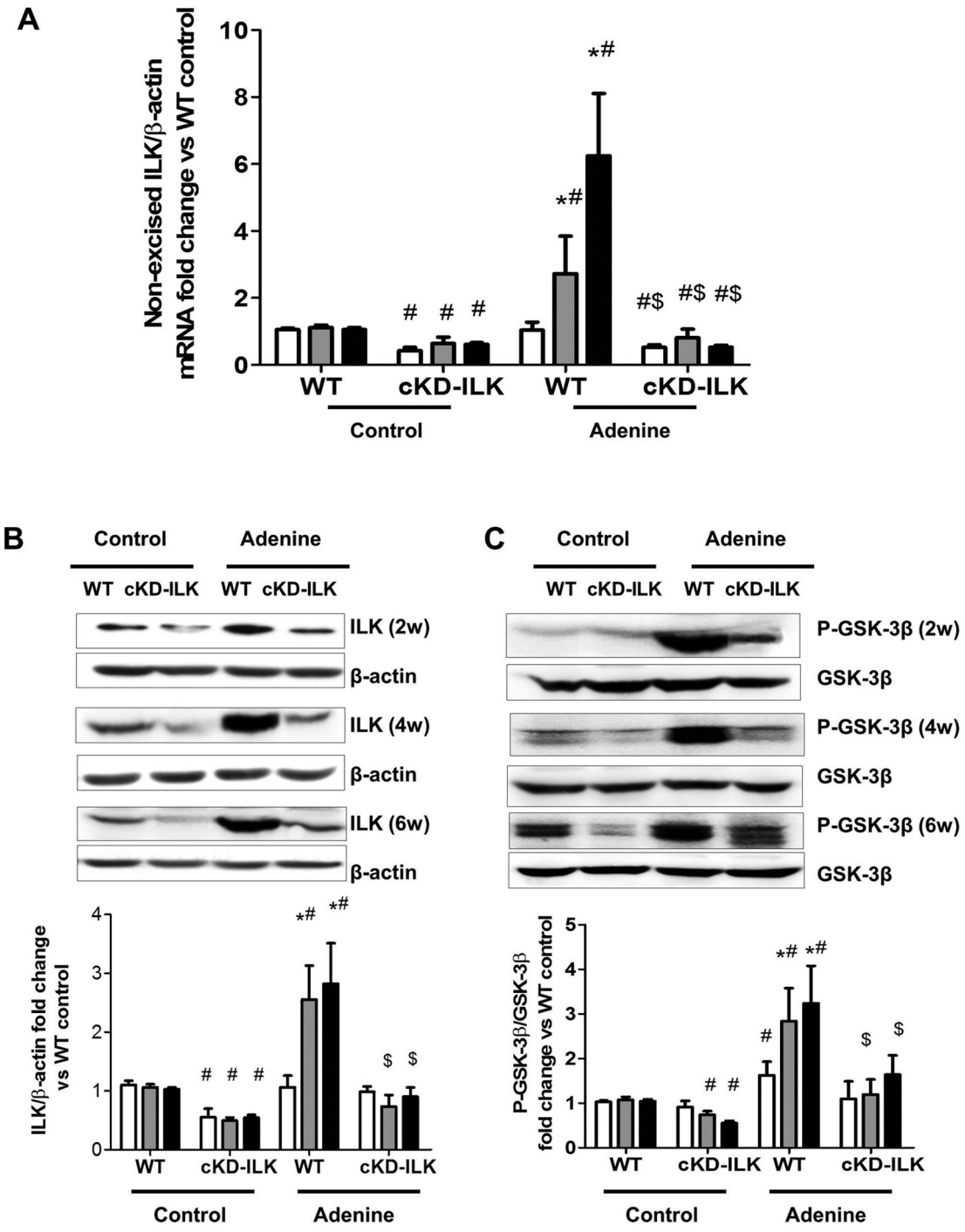

Fig. 4. ILK content and activity increase in the renal cortex of adenine-fed mice.
Wild type (WT) and ILK conditional-knockdown (cKD-ILK) mice were fed an adenine-rich or standard (controls) diet for 2 (2w; white bars), 4 (4w; gray bars) or 6 (6w; black bars) weeks and renal cortex samples were analyzed. Non-excised ILK (A) mRNA expression and (B) relative fold changes in protein content vs. the same week WT control normalized against β-actin as the endogenous control. (C) Phosphorylated GSK-3β in residue serine-9 (P-GSK-3β) protein content analysis normalized against total GSK-3β as endogenous controls. Representative blots and normalized densitometry analysis of the blots are shown. n = 10 animals/group. Results are shown as mean ± SEM. *P < 0.05 vs. 2 weeks, #P < 0.05 vs. WT or cKD-ILK controls at the same time, $P < 0.05 vs. WT Adenine at the same time.

collagens that are present in renal fibrosis and ECM protein sequences modulate the ILK activity that increases TGF-β1 expression in smooth muscle cells and glomerular mesangial cells, which finally perpetuates ECM production [27–29].

We demonstrated that ILK plays a key role in the regulation of Angiotensin II-induced or cisplatin-induced renal inflammation [25,30], as suggested in other inflammatory contexts [31,32].

Together, these results underscore the potential importance of ILK as a crucial regulator during the pathogenesis of tissue inflammation and fibrosis. Thus, it is conceivable to speculate that the depletion of ILK might block the initiation of the EMT conversion, as well as inflammation and fibrosis; thereby, preventing the progression of CKD.

In the present work, we used ILK conditional-knockdown mice (cKD-ILK) [25,30] to evaluate 1) whether ILK could be involved in CKD progression and 2) the consequences of ILK abrogation in an experimental model of progressive CKD. In order to do this study, the animals

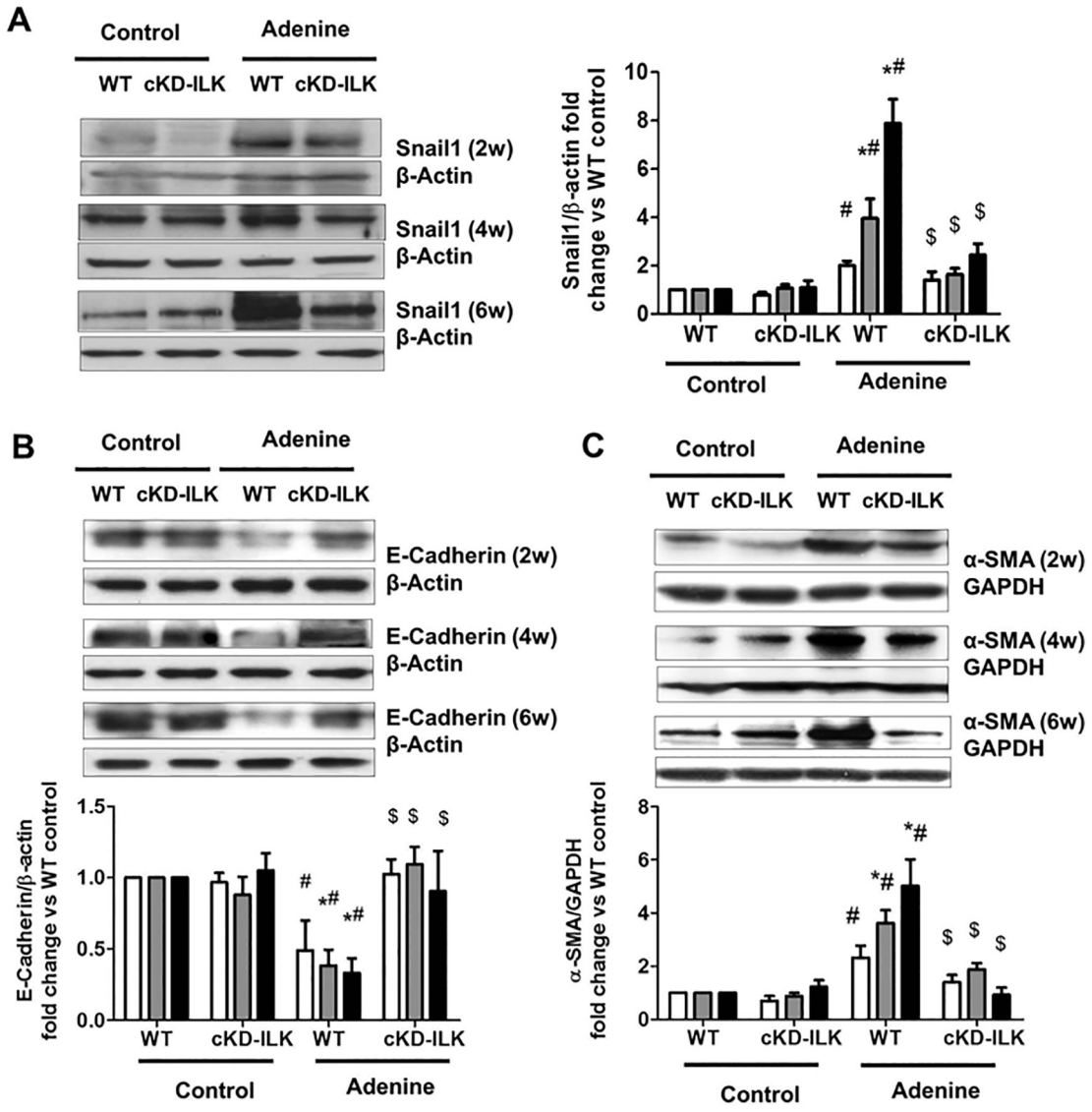

Fig. 5. ILK depletion inhibits Snail1 and α-SMA overexpression and prevents E-cadherin downregulation in the renal cortex of adenine-fed mice.
Wild type (WT) and ILK conditional-knockdown (cKD-ILK) mice were fed an adenine-rich or standard (controls) diet for 2 (2w; white bars), 4 (4w; gray bars) or 6 (6w; black bars) weeks and renal cortex samples were analyzed. (A) Snail1, (B) E-Cadherin and (C) relative fold changes in α-SMA protein content vs. the same week WT control normalized against β-actin or GAPDH as endogenous control, respectively. Representative blots and normalized densitometry analysis of the blots are shown. Results are shown as mean ± SEM. *P < 0.05 vs. 2 weeks, #P < 0.05 vs. WT or cKD-ILK controls at the same time, $P < 0.05 vs. WT Adenine at the same time. (n = 10 animals/group).

were subjected to an adenine-rich diet that induced renal damage and resembled the uremic features that are present in human CKD [33–35]. Additionally, 3) we also evaluated the potential role of ILK depletion as a therapeutic procedure to be applied after the disease induction, as a more effective approach in the interventions of human CKD subjects. Our results show that ILK may be critical during CKD pathophysiology and progression and therefore the ILK blockade could be a useful therapeutic strategy against CKD.

2. Materials and methods

2.1. Reagents

All culture reagents including FBS and antibiotics, lipofectamine, RNAlater solution, TRIzol, High Capacity cDNA Reverse Transcription Kit, SYBR Green Master Mix were from Life Technologies (Carlsbad, CA, USA). TGF-β1 and E-Cadherin antibodies were from Santa Cruz Biotechnology (Santa Cruz, CA, USA) and fibronectin, collagen type I (COL I) and Snail 1 antibodies and Sodium Assay Kit were from Abcam (Cambridge, UK). Anti-rabbit antibody was from Dako (Barcelona, Spain). Chemiluminescence reagent was from Thermo Scientific (Basingstoke, UK). The FastStart DNA Master SYBR Green I Kit was from Roche (Mannhein, Germany). Adenine, histology reagents, tamoxifen and other reagents and α-SMA antibody were from Sigma-Aldrich Chemical Company (St. Louis, MO, USA).

2.2. cKD-ILK mice

All procedures involving animals were approved by the Institutional Animal Care and Use Committee of the University of Alcalá and conformed to Directive 2010/63/EU of the European Parliament. The setting of the cKD-ILK transgenic model has been implemented previously by us [25,30,36]. Briefly, global, conditional inactivation of the ILK gene was accomplished by crossing C57Bl/6 mice homozygous for floxed ILK flanked by loxP (LOX mice), with mice homozygous for tamoxifen (TX)-inducible CreER(T) recombinase (CRE mice). Male CRE-

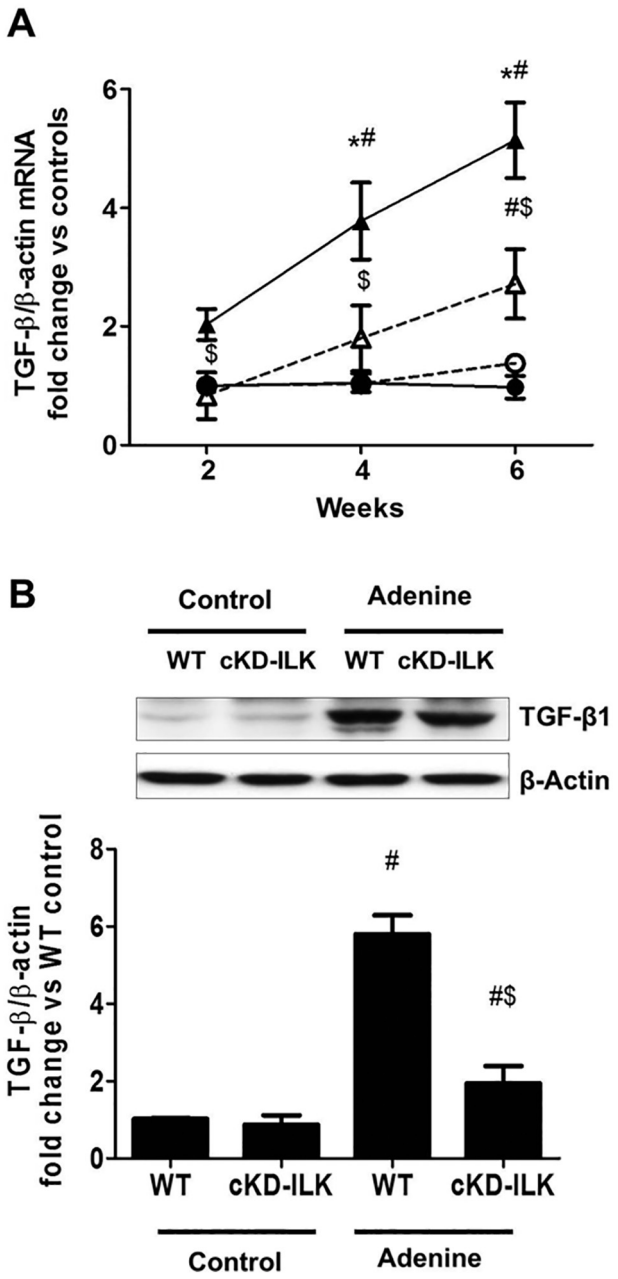

Fig. 6. ILK depletion prevents TGF-β1 overexpression in the renal cortex of adenine-fed mice.
Wild type (WT, continuous lines, black symbols) and ILK conditional-knockdown (cKD-ILK, dashed lines, open symbols) mice were fed an adenine-rich (triangles) or standard diet (controls, circles) during 2, 4 or 6 weeks and renal cortex samples were analyzed. TGF-β1 (A) mRNA expression and (B) 6th week relative fold changes in protein content vs. control WT normalized against β-actin as endogenous control. Representative blots and normalized densitometry analysis of the blots are shown. n = 10 animals/group. Results are shown as mean ± SEM. *P < 0.05 vs. 2 weeks, #P < 0.05 vs. WT or cKD-ILK controls at the same time, $P < 0.05 vs. WT Adenine at the same time.

LOX mice (8-week-old) were injected intraperitoneally with 1.5 mg of TX or vehicle (VH), once per day for 5 consecutive days, to induce ILK deletion. 3 weeks after the injections, tail DNA was genotyped by PCR with primers corresponding to excised ILK gene (230 bp) or to non-excised ILK (2100 bp): CCAGGTGGCAGAGGTAAGTA and CAAGGAAT AAGGTGAGCTTCAGAA [25,30,36,37]. The TX-treated CRE-LOX mice displaying successful depletion of ILK were termed cKD-ILK mice, and the VH-treated CRE-LOX mice were termed wild-type (WT) (Supplementary Fig. 1).

2.3. CKD in mice model and study design

After the ILK depletion period, WT and cKD-ILK mice control groups were fed a standard pellet chow throughout experimentation. For the induction of CKD, WT and cKD-ILK mice were bred as littermate controls and fed a 0.2% adenine-containing diet during 2, 4 or 6 weeks [33–35].

For the "clinical approach" study, the animals were fed an adenine-containing diet for 2 weeks, and after that, the ILK depletion was performed as described above. The animals were fed the adenine-containing diet 4 weeks more. Body weights were recorded daily. Basal (0 week), or 2- and 4-week blood samples were collected by incision of an inferior palpebral vein. All other parameters were analyzed at 0, 2, 4 and 6 weeks of the experimental period, when mice were sacrificed. One day before sacrifice, the animals were housed in metabolic cages to collect 24 h urine. At 24 h, the mice were anaesthetized with ketamine-xylazine (100/20 mg/kg, intraperitoneally), subjected to a thoracotomy and then exsanguinated through a right atrial cut. Both kidneys were removed, one fixed in buffered 10% formaldehyde solution for histological analysis and the other kidney stored in RNA later at −80 °C for RT–qPCR assays.

2.4. Clinical and biochemistry

Blood pressure was measured in conscious mice placed on a heated platform (Hatteras Instruments, Cary, NC, USA) using a tail-cuff sphygmomanometer (LE 5001 Pressure Meter, Letica Scientific Instruments, Hospitalet, Spain). Data were recorded before and after adenine treatment. Blood pressure was considered as the mean of at least twenty consecutive valid measurements. All mice were trained with the tail-cuff system [36]. At 0, 2, 4 and 6 weeks, biochemical analyses were performed in blood samples collected from mice fasted for 8–12 h. Serum was separated by centrifugation at 5000 rpm and stored at −80 °C until assayed. Plasma and urine creatinine and blood urea nitrogen (BUN) were determined with commercial kits according to the manufacturer's protocol (Arbor Assays LLC Ann Arbor, MI, USA). Plasma and urine sodium ion concentration was detected using Sodium Assay Kit and the Fractional excretion of Na (FENa) was calculated. From this point on, every spectophotometry determination was achieved with the Multimode Plate Reader Victor X4 (PerkinElmer, Waltham, MA, USA).

2.5. In vitro cultured HK2 and mIMCD3 cells

Human kidney tubular epithelial cell line (HK2) was purchased from American Type Culture Collection (ATCC, Rockville, MD, USA), maintained in DMEM supplemented with hydrocortisone, Insulin-Transferrine-Selenium, non-essential amino acids, penicillin, streptomycin and 10% FBS. Murine inner medullary collecting duct epithelial cell line (mIMCD3) was purchased from ATCC, maintained in supplemented DMEM-F12. Cells were routinely cultured in 95% air, 5% CO_2, at 37 °C. Confluent cells were serum-deprived for 24 h before adenine treatment (200–4800 μM). 24 h after the treatments, ILK, GSK-3β phosphorylation, GSK total content, TGF-β1, fibronectin and COL I contents were analyzed by RT-qPCR or immunoblots as described below.

Reverse transcription– quantitative polymerase chain reaction (RT-qPCR).

Total RNA from each sample was extracted with TRIzol, transcribed to cDNA with a high capacity cDNA RT kit, and 10 ng cDNA were amplified by TaqMan qPCR gene expression assays for MCP-1, total ILK and β-actin. To quantify non-excised ILK mRNA, RT-qPCR analysis was performed with SYBR Green Master Mix with primers GGGCTCTTGT GAGCTTCTGT and GAGTGGTCCCCTTCCAGAAT, designed to recognize

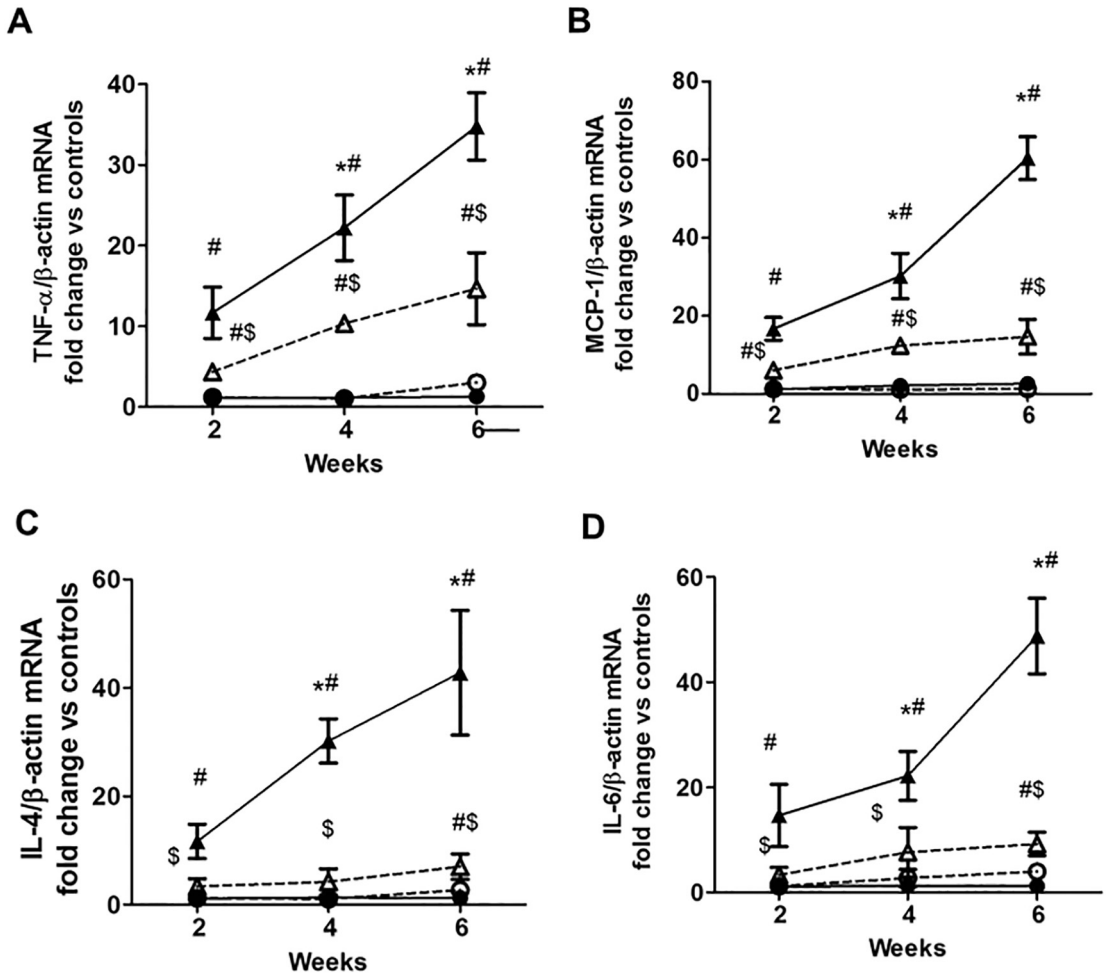

Fig. 7. ILK deletion prevents inflammatory gene overexpression in the renal cortex of adenine-fed mice.
Wild type (WT, continuous lines, black symbols) and ILK conditional-knockdown (cKD-ILK, dashed lines, open symbols) mice were fed an adenine-rich (triangles) or standard diet (controls, circles) during 2, 4 or 6 weeks and renal cortex samples were analyzed. (A) TNF-α, (B) MCP-1, (C) IL-4 and (D) relative fold changes in IL-6 mRNA expression vs. control WT are represented after the normalization with total β-actin content as the endogenous control. Results are shown as mean ± SEM. *P < 0.05 vs. 2 weeks, #P < 0.05 vs. WT or cKD-ILK controls at the same time, $P < 0.05 vs. WT Adenine at the same time. (n = 10 animals/group).

the cDNA sequence between exons within floxed areas 6 and 7 [25]. For the other genes, primers, designed using the PUBMED Gene Database, were: TGF-β1, 5′-TTGCTTCAGCTCCACAGAGA-3′ (forward) and 5′-TGGTTGTAGAGGGCAAGGAC-3′ (reverse); fibronectin, 5′-TGAGCG CCCTAAAGATTCCA-3′ (forward) and 5′-TAGCCACCAGTCTCATG TGC-3′ (reverse); COL I, 5′-TCCTGGCAACAAAGGAGACA-3′ (forward) and 5′-GGGCTCCTGGTTTTCCTTCT-3′ (reverse); TNF-α, 5′- TGGCCCA GACCCTCACACTCA-3′ (forward) and 5′- GGCTCAGCCACTCCAGC TGC-3′ (reverse); IL-6, 5′- CCGGAGAGGAGACTTCACAGAGGA-3′ (forward) and 5′- AGCCTCCGACTTGTGAAGTGGTATA-3′ (reverse); IL-4, 5′-ACAGGAGAAGGGACGCCAT-3′ (forward) and 5′-GAAGCCCTACAG ACGAGCTCA-3′ (reverse); β-actin, 5′-GACGGCCAGGTCATCACTAT-3′ (forward) and 5′-CTTCTGCATCCTGTCAGCAA-3′ (reverse). Results are expressed as fold increase using the ΔΔCt method normalized to β-actin [25].

2.6. Western blot analysis

Tissues or cells were lysate and protein samples were run on SDS-PAGE gels and transferred to polyvinylidene difluoride membranes. After membranes were blocked, immunodetection was performed with antibodies anti- ILK, P-GSK-3β(Ser9), GSK-3β, TGF-β1, Snail 1, E-Cadherin, α-SMA, fibronectin and COL I, followed by HRP-conjugated secondary antibodies. Antibody-bound proteins were visualized by chemiluminescence (ECL, Amersham, Little Chalfont, UK) [38]. Densitometry analyses were performed using ImageJ software (National Institutes of Health, USA).

2.7. Histology

Kidney tissue was fixed in 4% PFA, dehydrated and embedded in paraffin. Kidney sections were stained with Hematoxylin-eosin and Periodic acid-Schiff stain (PAS) according to the manufacturer's instructions. Histopathological features were determined based on quantitatively different scores: grade 0; affecting 0–5% of the renal area, grade 1; 6–25%, grade 2; 26–50%, and grade 3; > 50%. Several parameters were included in this analysis, such as tubular dilatation, loss of tubular epithelial cells, loss of brush border in proximal tubules, tubular apoptosis, tubular atrophy, pus casts in tubules and interstitial inflammation. Interstitial fibrosis was assessed by Sirius red staining of the collagen renal cortex content. Paraffin kidney sections (2–3 μm) were incubated with Sirius red solution for 60 min, washed in acidified water, dehydrated in ethanol, cleared in xylene and mounted in DPX. 8 random fields from each renal cortex section were photographed and the positive areas were calculated using ImageJ plus software (National Institutes of Health, USA). All morphological analyses were performed blindly by two different experienced pathologists [25,30,38].

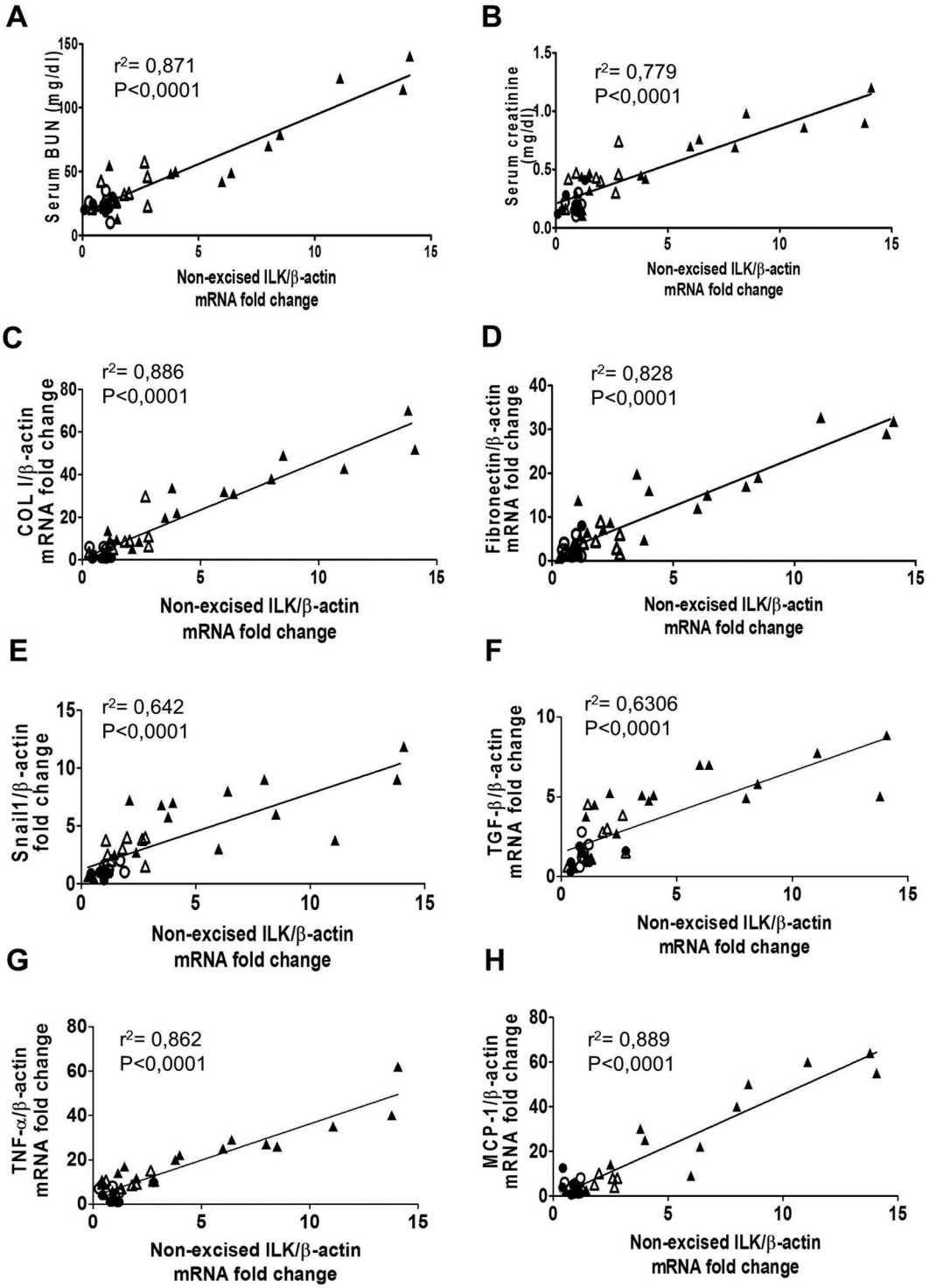

Fig. 8. Analysis of the co-relations between renal cortex ILK mRNA levels and the renal function or expression of markers related to fibrosis, EMT, and inflammation. Wild type (WT, black symbols) and ILK conditional-knockdown (cKD-ILK, open symbols) mice were fed an adenine-rich diet (triangles) or standard diet as control (circles) during 6 weeks. Renal cortex ILK mRNA levels were confronted to the values obtained in the previous figures: (A) blood urea nitrogen (BUN) and (B) creatinine (mg/dl), (C) Collagen I (COL I), (D) fibronectin mRNA expressions, (E) Snail1 protein content, (F) TGF-β1, (G) TNF-α and (H) MCP-1 mRNA expressions. The analysis is detailed in the Materials and methods section.

2.8. Statistical analysis

All data were analyzed using GraphPad software (La Jolla, CA, USA). Results are expressed as mean ± SEM, except for histopathological feature data, which are presented as median and quartile ranges. As the number of animals or samples in the different experiments was never over 10, non-parametric statistics were used for comparisons, applying the Kruskal-Wallis with Mann-Whitney post-test (non-paired data) or Friedman with Wilcoxon post-test (paired data). Correlation analysis between ILK mRNA renal levels and serum BUN and creatinine or Snail1, TGF-β1, COL I, Fibronectin, TNF-α and MCP-1 renal levels was performed using linear regression for each genotype (combining

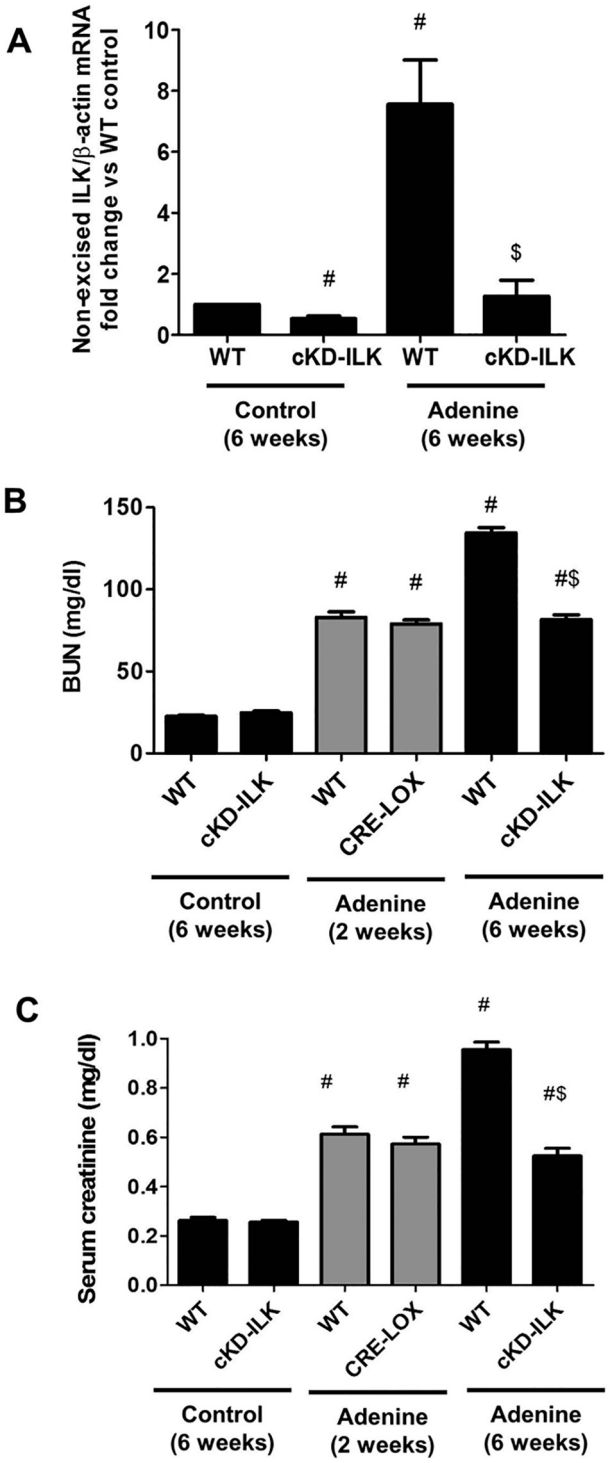

Fig. 9. ILK depletion during the progression of CKD prevents renal function decrease.

CRE-LOX mice were fed an adenine-rich or standard (controls) diet for 2 weeks. ILK depletion was induced at that moment, and the animals with (cKD-ILK) or without ILK-depletion (WT) continued on the same diet for 4 additional weeks. Blood samples were collected at the 2nd and 6th week. Renal cortex samples were analyzed at the 6th week. (A) Fold changes in non-excised ILK mRNA expression in the renal cortex vs. the control WT normalized against β-actin as the endogenous control. Renal function was assessed by measuring 2nd and 6th week (B) blood urea nitrogen (BUN) and (C) creatinine (mg/dl). n = 8 animals/group. Results shown are the mean ± SEM. $^{\#}P < 0.05$ vs. WT or cKD-ILK controls at the same time, $^{\$}P < 0.05$ vs. WT Adenine at the same time.

WT Control, cKD-ILK Control, WT Adenine and cKD-ILK Adenine treatment) and plotted on the same graph. A value of $P < 0.05$ was considered to be statistically significant.

3. Results

3.1. The adenine-induced mouse model of CKD shows increased ILK expression and activity in the kidney

Previous studies pointed out that the rodent model induced by an adenine-enriched diet developed chronic kidney damage [33–35]. Our mice were fed this diet and analyzed at the 2nd, 4th and 6th weeks of treatment. Adenine-fed WT mice exhibited body weight reduction (starting at the 2nd week of the diet administration) and became hypertensive (starting at the 4th week) (Table 1). 20–30% reduction of food intake was observed, and the mortality was similar in the different groups studied (about 5%, data not shown). In addition, kidneys from adenine-fed mice were found to be significantly smaller, with around 13% of size reduction at the 6th week of treatment.

A progressive decline of renal function appeared in the adenine-fed WT as early as the 2nd week of treatment (Fig. 1), with increased BUN and creatinine serum concentrations (Fig. 1, panels A and B), as well as disturbances in the tubular management of sodium and water, manifested by an increased Fractional excretion of Na (FENa) and urinary volume (Fig. 1, panels C and D).

In addition to the changes in renal function, the 6-week adenine-fed WT exhibited significant renal tubule-interstitial changes and none glomerular lesions were observed (Fig. 2 and Table 2). The pathological analysis of the kidneys showed significant tubular lesions, such as deposition of 2,8-dihydroxyadenine (DHOA) crystals in the tubular compartment, marked tubular dilatation, loss of tubular epithelial cells and brush border membranes in proximal tubules, tubular apoptosis, tubular atrophy, intra-tubular pus casts and accumulation of inflammatory cells at the interstitial compartment (Fig. 2, Table 2).

Increased fibrosis was markedly and progressively induced by the adenine-rich diet in WT as early as the 2nd week of treatment, according to the results observed in the histological studies (Fig. 2, Table 2) and confirmed by the analysis of the renal mRNA and protein contents of ECM components COL I (Fig. 3A and B) and fibronectin (Fig. 3C and D).

ILK expression (mRNA and protein contents) progressively increased in the renal cortex of adenine-fed WT mice (Fig. 4A and B), being statistically significant at the 4th week of treatment. Accordingly, the ILK activity, determined by the increased phosphorylation level of GSK-3β at serine-9 [14,37,39], started to increase at the 2nd week of adenine treatment (Fig. 4C).

To rule out that ILK changes could be caused by the direct adenine effect on tubular cells, two tubular cell lines (human kidney tubular epithelial HK2 and murine inner medullary collecting duct epithelial mIMCD3) were treated in vitro with increasing adenine concentrations, ranging from 200 to 4800 μM. These in vitro treatments were nontoxic (data not shown) and did not affect either ILK expression or activity in any of the cell lines (Supplementary Fig. 2A to D).

3.2. ILK depletion prevents the progression of induced chronic kidney damage in mice

Like WT mice, their cKD-ILK littermates (mice displaying successful depletion of ILK) were also subjected to the same adenine-enriched diet. In cKD-ILK mice, the transgenic depletion of ILK resulted in a significant decrease in non-excised ILK mRNA and protein contents and in the activity in cKD-ILK renal cortex from 0 to 6 weeks of adenine treatment (Fig. 4). Blood pressure (Table 1), serum BUN, creatinine, FENa and urinary volume significantly decreased in adenine-fed cKD-ILK mice compared to adenine-fed WT ones, although they did not reach the WT control values (Fig. 1). ILK depletion protected against the progressive

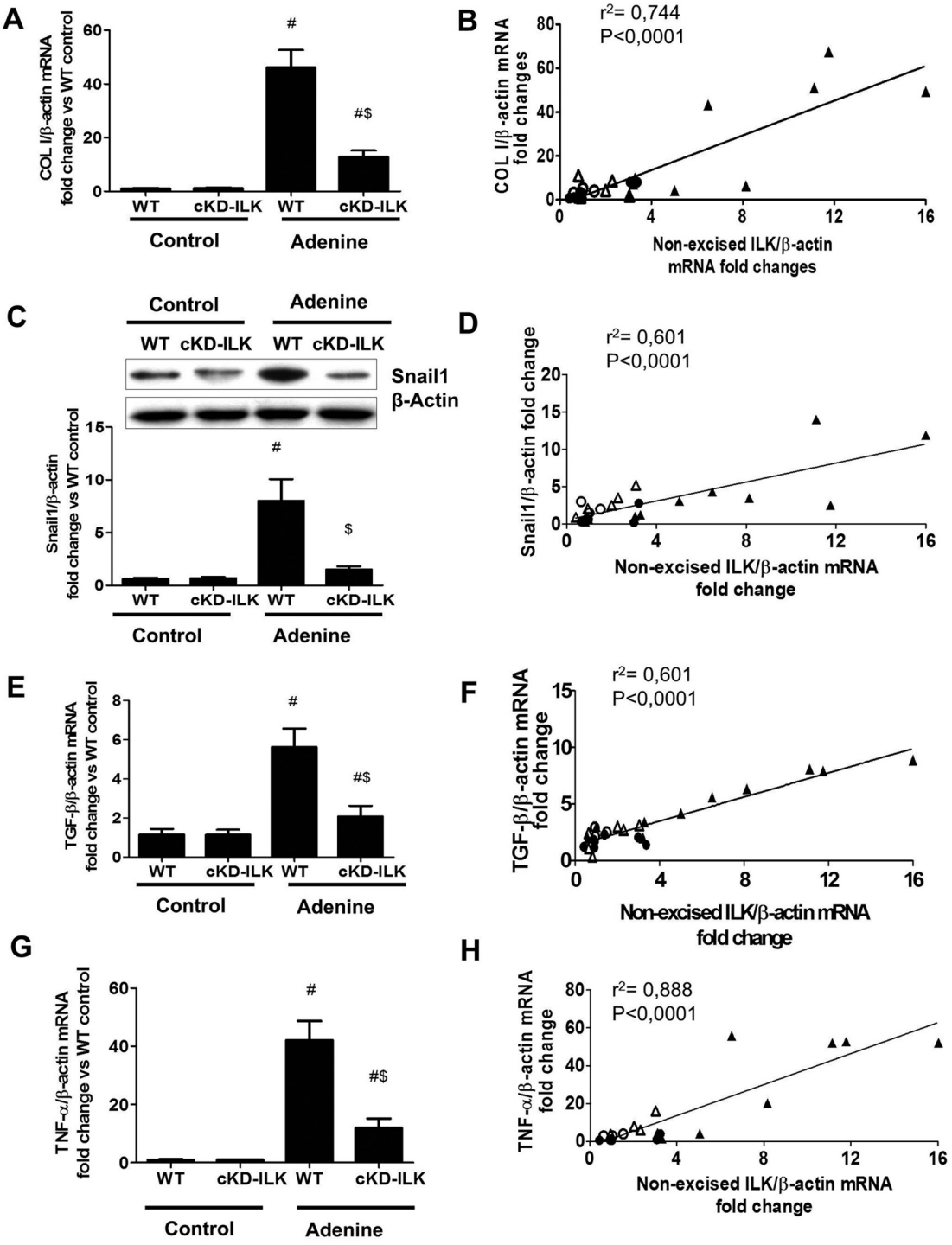

Fig. 10. ILK depletion during the progression of CKD prevents the expression of markers related to fibrosis, EMT, and inflammation.
CRE-LOX mice were fed an adenine-rich or standard (controls) diet for 2 weeks. ILK depletion was induced at that moment. The animals with (cKD-ILK) or without ILK- depletion (WT) continued on the same diet for 4 additional weeks. The renal cortex was analyzed at the 6th week. (A) Collagen I (COL I), (E) TGF-β and (G) TNF-α mRNA expression and (C) Snail1 protein content were quantified in the renal cortex at the 6th week of treatment. Relative fold changes in mRNA or protein content vs. control WT are represented after the normalization with total β-actin content as the endogenous control. n = 8 animals/group. Results shown are the mean ± SEM. $^{\#}P < 0.05$ vs. WT or cKD-ILK controls, $^{\$}P < 0.05$ vs. WT Adenine. (B, D, F and H) the co-relations between non-excised ILK mRNA levels in renal cortex at the 6th week shown in the previous figure and the expression of the markers.

tubule-interstitial injury caused by the adenine diet. When compared to WT mice with renal damage, cKD-ILK mice with adenine-induced chronic renal failure exhibited a significant decrease in tubular lesions, inflammation and fibrosis (Table 2 and Figs. 2 and 3). In order to rule out that the preventive modifications observed in mice with adenine-induced renal damage could be due to the tamoxifen administration itself on our cKD-ILK model, we administered tamoxifen to parental CRE and LOX mice (5 days of treatment, following the same experimental design described for CRE-LOX to induce ILK depletion). In these animals, ILK depletion was not induced, and the adenine diet produced the same structural and functional changes at renal level as in WT mice (data not shown). Finally, the depletion of ILK in cKD-ILK mice did not

affect the normal kidney structure and function in the animals that fed a standard diet (controls in Tables 1 and 2 and Figs. 1, 2 and 3).

3.3. ILK depletion provides mechanisms to protect against renal injury

To better understand the protection provided by ILK depletion on adenine-induced chronic renal failure, we explored the following mechanisms: first, as EMT may be involved in the development of tubule-interstitial renal damage, we analyzed the expression of EMT related markers in the renal cortex. In adenine-fed WT mice, we observed a significant and progressive increase in the transcription factor Snail1 expression, which had a slight progressive increase in the adenine-fed cKD-ILK ~~ones~~ (Fig. 5A). In adenine-fed WT, the overexpression of Snail1 resulted in down-regulation of the epithelial marker E-cadherin, and ILK depletion was able to restore the repressed E-cadherin expression since the beginning of the adenine treatment (Fig. 5B). We further examined the myofibroblast activation during the chronic renal damage induction. In adenine-fed WT mice, a progressive increase in the content of molecular hallmark α-smooth muscle actin (α-SMA) in myofibroblasts was observed, and the ILK depletion largely blocked this overexpression during the adenine treatment (Fig. 5C). The cytokine TGF-β1 is regarded as one of the most important mediators which regulates EMT and renal fibrosis. Adenine-fed WT mice exhibited a significant progressive increase in TGF-β1 mRNA expression in the renal cortex, as early as the 2nd week of treatment. The ILK depletion partially inhibited this effect throughout the treatment (Fig. 6A). Similarly, TGF-β1 protein content was also abrogated in cKD-ILK mice in the 6th week of adenine treatment (Fig. 6B). The adenine in vitro treatment of tubular cells HK2 and mIMCD3 did not modify the TGF-β1, COL I and fibronectin expression, which ruled out that adenine directly affected the expression of these fibrosis-related markers (Supplementary Fig. 3). Finally, we explored the potential anti-inflammatory effect of ILK depletion during the genesis and development of the adenine-induced chronic kidney damage. The renal mRNA expression of pro-inflammatory (TNF-α, IL-4, IL-6) and chemoattractant (MCP-1) cytokines significantly increased in the adenine-fed WT group, but not in the adenine-treated cKD-ILK mice (Fig. 7).

3.4. ILK content in the renal cortex directly correlates with plasma BUN and creatinine, as well as with cortical ECM proteins, EMT markers, TGF-β1 and inflammatory cytokines expression

To better understand the pathophysiological relationship between ILK protein content and the renal expression of different markers that affect renal function, we evaluated the correlation of values. Interestingly, we found a high significance in the correlations between cortical ILK mRNA content and plasma BUN and creatinine, renal COL I, fibronectin, TGF-β1, TNF-α and MCP-1 mRNA levels and Snail1 protein content (Fig. 8). The r^2 coefficients are over 0.8 in most of the cases and P values are under 0.0001 in every case. These data suggest a potential direct relationship between renal ILK content and EMT, fibrosis and inflammation phenomena underlying CKD progression.

3.5. ILK depletion during the progression of CKD also prevents chronic renal damage induced by an adenine-rich diet

Any therapy used to treat patients suffering from CKD is administered once renal damage has been established and the aim of the therapy is to palliate the progression of the disease. In this context, we tested ILK depletion once the adenine-induced disease had already started. Thus, the animals were supplemented with an adenine-rich diet for 2 weeks and ILK-depleted at that moment, following the same transgenic induction with tamoxifen for 5 consecutive days, maintaining the adenine diet for 4 more additional weeks (a total of 6 weeks). At the end of the experiment, the analysis of non-excised ILK mRNA in the renal cortex confirmed the successful ILK depletion (Fig. 9A). All animals showed a significant elevation of BUN and creatinine levels in the 2nd week on the adenine diet. These parameters were further increased in the 6th week in the adenine-supplemented WT, but no progression was observed in the cKD-ILK group (Fig. 9, panels B and C). Furthermore, the ILK-depleted group completely prevented the increased expression of the markers COL I, TGF-β1, TNF-α and Snail1, with a highly significant statistical correlation between these parameters and ILK renal cortex content (Fig. 10).

We excluded tamoxifen administration as the cause of the effects observed by performing the same experimental model as above in parental CRE and LOX mice. The evolution of renal dysfunction (determined by plasma BUN and creatinine concentrations) in these mice was similar to adenine-fed WT (data not shown).

4. Discussion

In the present study, we assessed the key role of ILK in the genesis and progression of CKD by performing a mouse experimental model where we transgenically depleted ILK at the beginning as well as during the progression of the disease. Our results demonstrate that ILK expression in renal tissue increases as CKD progresses, and this increased ILK content correlates well with different molecules that are considered markers or pathogenic factors of renal damage. Finally, ILK depletion prevents renal disease progression. The contrasted experimental model chosen is based on the administration of high amounts of adenine in the diet [33–35], because adenine induces gradual and progressive kidney damage that allow us to analyze the consequences of ILK depletion through the progression of the disease.

The adenine is absorbed and metabolized into DHOA, an insoluble compound that precipitates in renal tubules, which promotes tubular occlusion and tubular epithelium physical injury. DHOA leads to the formation of intratubular casts, with extensive tubular dilation and secondary inflammation, necrosis, foreign-body granulomas and ultimately, tubule-interstitial fibrosis that consequently produce renal dysfunction, characterized by elevated levels of serum urea nitrogen and creatinine [33–35]. Some characteristics of this model resemble the diseases characterized by increased intratubular renal pressure (urologic diseases, chronic renal damage following acute tubular necrosis with intratubular casts) or intratubular accumulation of toxic metabolites or proteins (myeloma kidney, acute renal damage associated to very increased levels of uric acid), and even to the chronic kidney damage described as Mesoamerican nephropathy, that has been proposed to be due to intratubular crystal depositions linked to sustained and repeated dehydrations [40].

Our adenine-treated animals exhibited increased BUN (aprox 5-fold), creatinine (aprox 2-fold), and urine volume (aprox 6-fold). These changes are characteristic of patients with predominant tubule-interstitial damage in early-middle stages. Other authors have made similar approaches by studying animals fed with adenine for 1–2 week, as they were interested in inflammation as the initial event in the development of renal damage in this model [2], or in the prevention of the progression of the disease [41]. Longer treatment times, between 3 and 8 weeks, were selected by other authors more devoted to the analysis of established fibrosis [42,43]. Because we were interested both in the analysis of the mechanism of development/progression and in the prevention of the disease, we selected 2 to 6 weeks of treatment.

The functional changes previously mentioned, together with the structural abnormalities in the tubules showed in the Results section were observed in our adenine-fed animals, which exhibited a progressive increase in renal ILK content and activity. Similarly, increased levels of ILK were also observed in a wide variety of chronic kidney diseases in both experimental and clinical settings [16,18,20,21]. We observed that ILK overexpression was not the consequence of a direct effect of adenine on cells, as ILK protein content and activity did not change in tubular cells incubated directly with adenine, but probably of the complex interaction that took place at tubular level after DHOA

crystal deposition.

ILK can be a very interesting target to be analyzed during the progression of renal disease. Its involvement in the modulation of key mechanisms implicated in CKD, such as TGF-β expression and ECM protein accumulation [27–29,44], EMT induction [15–22,26], and activation of local inflammatory responses, as has been shown in vitro and in vivo by us and others [30]. Additionally, ILK is activated by the interaction of integrins with ECM proteins [27,29], accumulated during chronic renal fibrosis, and it could be proposed as a key molecule that determines and auto-perpetuates the mechanisms that contribute to CKD progression. In adenine-fed mice, we demonstrated the activation of many of the above-mentioned mechanisms and their inhibition conditioned by ILK depletion. Our excellent correlations between renal ILK content and the different parameters tested reinforce the hypothesis that ILK can be considered a good therapeutic target.

Several authors have observed that ILK regulating action of EMT is mediated by its protein kinase activity, because an ILK kinase-dead mutant and specific kinase inhibitor block TGF-β-mediated EMT in vitro or renal interstitial fibrosis in obstructive nephropathy [15,16,19]. Our results do not clarify whether the loss of ILK scaffolding function or its kinase activity is responsible for the blockade of the pathogenic mechanisms previously mentioned.

Before our study, other groups attempted to inhibit ILK at kidney level, which becomes a complex methodological problem; ILK has no safe pharmacological inhibitors available. Li and coauthors [22] tested the effect of a potential candidate molecule, QLT-0267, but on a short-term basis. Transgenic mice with specific podocytes ILK deletion exhibited a progressive focal segmental glomerulosclerosis, massive proteinuria and premature death [45]. Our present work used an adult transgenic model of general ILK depletion, which showed a sustained decrease in ILK in kidney cells (from 1 to 3 months after 5 days of tamoxifen treatment) with normal renal function that includes normal histological appearance of renal structures and urine protein excretion [25,32].

The possibility that tamoxifen, and not ILK, could be responsible for renal function improvement seems improbable because the treatment with tamoxifen given to CKD was discontinued and adequate excluding control experiments were performed [46].

Experiments done to block particular proteins prior to the development of the disease in an animal model, in whichever context, are relevant to understand the pathophysiology and to indicate if the protein can be used as a therapeutic target. Yet, these experiments are far from reproducing any strategies deemed necessary for the clinical management of human disease. In fact, patients are referred to medical care when renal diseases are established and treatments must prove to be safe and effective at these stages. In the present work, some of our results highlight the role of ILK during the development of adenine-induced kidney damage. Indeed, we also reproduced the hypothetical clinical situation where animals were depleted of their ILK two weeks after adenine-based CKD induction. In this clinical context approach, the beneficial effects mentioned were also achieved during the disease progression and excellent correlations between renal ILK content and the different parameters tested were again observed.

Our in vivo model confirmed the key role of ILK during the pathogenesis of some forms of renal diseases [17,22], but we explained some of the mechanisms involved in this process and verified for the first time that ILK blockade in the CKD early stages may stop the pathophysiological process that leads to the progression of renal disease to end-stage renal failure, which emphasizes great potential applications in clinical practice. Additional studies must be performed to determine whether these events are significant in some renal diseases or if they may be considered a mechanism of progression of renal damage.

Supplementary data to this article can be found online at https://doi.org/10.1016/j.bbadis.2019.01.024.

Transparency document

The Transparency document associated with this article can be found, in online version.

Acknowledgements

This work was supported by co-founded grants from the Instituto de Salud Carlos III (ISCIII) and FEDER funds (PI14/01939, PI14/02075, PI17/01513, PI17/00625, B2017/BMD-3751), the FEDER and ISCIII RETIC REDinREN programs (RD12/0021/0006 and RD16/0009/0018), University of Alcalá funds (CCG2015/BIO-034 and CCG2016/BIO-043) and Fundación Senefro (Senefro-2016), Instituto de Investigaciones Sanitarias Reina Sofía (IRSIN) and Fundación Renal Iñigo Álvarez de Toledo (FRIAT) funds.

Disclosures

None.

References

[1] W.G. Couser, G. Remuzzi, S. Mendis, et al., The contribution of chronic kidney disease to the global burden of major noncommunicable diseases, Kidney Int. (12) (2011) 1258–1270.
[2] C.F. Aguiar, C. Naffah-de-Souza, A. Castoldi, et al., Administration of α-galactosylceramide improves adenine-induced renal injury, Mol. Med. 21 (2015) 553–562.
[3] L.A. Stevens, J. Coresh, T. Greene, A.S. Levey, Assessing kidney function: measured and estimated glomerular filtration rate, N. Engl. J. Med. 354 (2006) 2473–2483.
[4] M.T. Grande, J.M. Lopez-Novoa, Fibroblast activation and myofibroblast generation in obstructive nephropathy, Nat Rev Nephrol 5 (2009) 319–328.
[5] M. Iwano, D. Plieth, T.M. Danoff, et al., Evidence that fibroblasts derive from epithelium during tissue fibrosis, J. Clin. Invest. 110 (2002) 341–350.
[6] M.T. Grande, B. Sánchez-Laorden, C. López-Blau, et al., Snail1-induced partial epithelial-to-mesenchymal transition drives renal fibrosis in mice and can be targeted to reverse established disease, Nat. Med. 21 (2015) 989–997.
[7] S. Lovisa, V.S. LeBleu, B. Tampe, et al., Epithelial-to-mesenchymal transition induces cell cycle arrest andparenchymal damage in renal fibrosis, Nat. Med. 21 (2015) 998–1009.
[8] M.A. Nieto, R.Y. Huang, R.A. Jackson, J.P. Thiery, EMT: 2016, Cell 166 (1) (2016) 21–45.
[9] G.E. Hannigan, C. Leung-Hagesteijn, L. Fitz-Gibbon, et al., Regulation of cell adhesion and anchorage-dependent growth by a new beta 1-integrin linked protein kinase, Nature 379 (1996) 91–96.
[10] C. Wu, S. Dedhar, Integrin-linked kinase (ILK) and its interactors: a new paradigm for the coupling of extracellular matrix to actin cytoskeleton and signaling complexes, J. Cell Biol. 155 (2001) 505–510.
[11] K.R. Legate, E. Montañez, O. Kudlacek, R. Fässler, ILK, PINCH and parvin: the tIPP of integrin signalling, Nat Rev Mol Cell Biol 7 (2006) 20–31.
[12] E. Boulter, E. Van Obberghen-Schilling, Integrin-linked kinase and its partners: a modular platform regulating cell-matrix adhesion dynamics and cytoskeletal organization, Eur. J. Cell Biol. 85 (2006) 255–263.
[13] G. Hannigan, A.A. Troussard, S. Dedhar, Integrin-linked kinase: a cancer therapeutic target unique among its ILK, Nat. Rev. Cancer 5 (2005) 51–63.
[14] A. García-Jérez, A. Luengo, J. Carracedo, et al., Effect of uraemia on endothelial cell damage is mediated by the integrin linked kinase pathway, J. Physiol. 593 (3) (2015) 601–618.
[15] S. Kagami, M. Shimiz, S. Kond, et al., Up-regulation of integrin-linked kinase activity in rat mesangioproliferative glomerulonephritis, Life Sci. 78 (2006) 1794–1800.
[16] M. Kretzler, V.P. Teixeira, P.G. Unschuld, et al., Integrin-linked kinase as a candidate downstream effector in proteinuria, FASEB J. 15 (2001) 1843–1845.
[17] Y.S. Kang, Y. Li, C. Dai, et al., Inhibition of integrin-linked kinase blocks podocyte epithelial-mesenchymal transition and ameliorates proteinuria, Kidney Int. 78 (2010) 363–373.
[18] P. Teixeira V de, S.M. Blattner, M. Li, et al., Functional consequences of integrin-linked kinase activation in podocyte damage, Kidney Int. 67 (2005) 514–523.
[19] M. Du, Q. Wang, W. Li, et al., Overexpression of FOXO1 ameliorates the podocyte epithelial-mesenchymal transition induced by high glucose in vitro and in vivo, Biochem. Biophys. Res. Commun. 471 (4) (2016) 416–422.
[20] L. Guo, P.W. Sanders, A. Woods, C. Wu, The distribution and regulation of integrin-linked kinase in normal and diabetic kidneys, Am. J. Pathol. 159 (2001) 1735–1742.
[21] Y. Li, J. Yang, C. Dai, et al., Role for integrin-linked kinase in mediating tubular epithelial to mesenchymal transition and renal interstitial fibrogenesis, J. Clin. Invest. 112 (2003) 503–516.
[22] Y. Li, X. Tan, C. Dai, et al., Inhibition of integrin-linked kinase attenuates renal interstitial fibrosis, J. Am. Soc. Nephrol. 20 (9) (2009) 1907–1918.
[23] B.C. Liu, M.X. Li, J.D. Zhang, et al., Inhibition of integrin-linked kinase via a siRNA

expression plasmid attenuates connective tissue growth factor-induced human proximal tubular epithelial cells to mesenchymal transition, Am. J. Nephrol. 28 (2008) 143–151.
[24] H.Y. Dai, M. Zheng, L.L. Lv, et al., The roles of connective tissue growth factor and integrin-linked kinase in high glucose-induced phenotypic alterations of podocytes, J. Cell. Biochem. 113 (2012) 293–301.
[25] J.L. Cano-Peñalver, M. Griera, A. García-Jerez, et al., Renal integrin-linked kinase depletion induces kidney cGMP axis upregulation: consequences on basal and acutely damaged renal function, Mol. Med. (2015), https://doi.org/10.2119/molmed.2015.00059.
[26] M.K. Kim, Y.I. Maeng, W.J. Sung, et al., The differential expression of TGF-β1, ILK and wnt signaling inducing epithelial to mesenchymal transition in human renal fibrogenesis: an immunohistochemical study, Int. J. Clin. Exp. Pathol. 6 (9) (2013) 1747–1758.
[27] R. Ortega-Velazquez, M.L. Diez-Marques, M.P. Ruiz-Torres, et al., Arg-Gly-Asp-Ser (RGDS) peptide stimulates transforming growth factor–beta1 transcription and secretion through integrin activation, FASEB J. 7 (2003) 1529–1531.
[28] R. Ortega-Velazquez, M. Gonzalez-Rubio, M.P. Ruiz-Torres, et al., Collagen I up-regulates extracellular matrix gene expression and secretion of TGF-beta 1 by cultured human mesangial cells, Am J Physiol Cell Physiol 286 (6) (2004) C1335–C1343.
[29] M.P. Ruiz-Torres, G. Perez-Rivero, M.L. Diez-Marques, et al., Role of activator protein-1 on the effect of arginine-glycine-aspartic acid containing peptides on transforming growth factor-beta1 promoter activity, Int. J. Biochem. Cell Biol. 39 (1) (2007) 133–145.
[30] M. Alique, E. Civantos, E. Sanchez-Lopez, et al., Integrin-linked kinase plays a key role in the regulation of angiotensin II-induced renal inflammation, Clin Sci (Lond) 127 (1) (2014) 19–31.
[31] K. Assi, J. Mills, D. Owen, et al., Integrin-linked kinase regulates cell proliferation and tumour growth in murine colitis-associated carcinogenesis, Gut 57 (2008) 931–940.
[32] K. Assi, S. Patterson, S. Dedhar, et al., Role of epithelial integrin-linked kinase in promoting intestinal inflammation: effects on CCL2, fibronectin and the T cell repertoire, BMC Immunol. 1 (2011) 12–42.
[33] T. Yokozawa, P.D. Zheng, H. Oura, et al., Animal model of adenine induced chronic renal failure in rats, Nephron 44 (1986) 230–234.
[34] A.C. Santana, S. Degaspari, S. Catanozi, et al., Thalidomide suppresses inflammation in adenine-induced CKD with uraemia in mice, Nephrol. Dial. Transplant. 28 (5) (2013) 1140–1149.
[35] M. Tamura, R. Aizawa, M. Hori, et al., Progressive renal dysfunction and macrophage infiltration in interstitial fibrosis in an adenine induced tubulointerstitial nephritis mouse model, Histochem. Cell Biol. 131 (2009) 483–490.
[36] I. Serrano, S. De Frutos, M. Griera, et al., ILK conditional deletion in adult animals increases cyclic GMP-dependent vasorelaxation, Cardiovasc. Res. 99 (2013) 535–544.
[37] A.A. Troussard, N.M. Mawji, C. Ong, et al., Conditional knock-out of integrin-linked kinase demonstrates an essential role in protein kinase B/Akt activation, J. Biol. Chem. 278 (2003) 22374–22378.
[38] P. Martín-Sánchez, A. Luengo, M. Griera, et al., H-ras deletion protects against angiotensin II-induced arterial hypertension and cardiac remodeling through protein kinase G-Iβ pathway activation, FASEB J. 32 (2) (2018) 920–934.
[39] M. Hatem-Vaquero, M. Griera, A. García-Jerez, et al., Peripheral insulin resistance in ILK-depleted mice by reduction of GLUT4 expression, J. Endocrinol. 234 (2) (2017) 115–128.
[40] C. Roncal-Jimenez, R. García-Trabanino, L. Barregard, et al., Heat stress nephropathy from exercise-induced uric acid crystalluria: a perspective on Mesoamerican nephropathy, Am. J. Kidney Dis. 67 (1) (2016) 20–30.
[41] S.C. Schiavi, W. Tang, C. Bracken, et al., Npt2b deletion attenuates hyperphosphatemia associated with CKD, J. Am. Soc. Nephrol. 23 (10) (2012) 1691–1700.
[42] S. Buchtler, A. Grill, S. Hofmarksrichter, et al., Cellular origin and functional relevance of collagen I production in the kidney, J. Am. Soc. Nephrol. 29 (7) (2018) 1859–1873.
[43] T. Jia, H. Olauson, K. Lindberg, et al., A novel model of adenine-induced tubulointerstitial nephropathy in mice, BMC Nephrol. 14 (2013) 116, , https://doi.org/10.1186/1471-2369-14-116.
[44] M. Gonzalez-Ramos, S. de Frutos, M. Griera, et al., Integrin-linked kinase mediates the hydrogen peroxide-dependent transforming growth factor-β1 up-regulation, Free Radic. Biol. Med. 61 (2013) 416–427.
[45] C. El-Aouni, N. Herbach, S.M. Blattner, et al., Podocyte-specific deletion of integrin-linked kinase results in severe glomerular basement membrane alterations and progressive glomerulosclerosis, J. Am. Soc. Nephrol. 17 (2006) 1334–1344.
[46] H. Dellê, J.R. Rocha, R.C. Cavaglieri, et al., Antifibrotic effect of tamoxifen in a model of progressive renal disease, J. Am. Soc. Nephrol. 23 (1) (2012) 37–48.